

# Electrical conductivity in graphene with point defects

Yuriy V. Skrypnyk<sup>1</sup> and Vadim M. Loktev<sup>2</sup>

<sup>1</sup>*G. V. Kurdyumov Institute of Metal Physics,*

*National Academy of Sciences of Ukraine Vernadsky Ave. 36, Kyiv 03680, Ukraine*

<sup>2</sup>*Bogolyubov Institute for Theoretical Physics,*

*National Academy of Sciences of Ukraine Metrolohichna Str. 14-b, Kyiv 03680, Ukraine*

## Abstract

The electrical conductivity of graphene containing point defects is studied within the binary alloy model in its dependence on the Fermi level position at the zero temperature. It is found that the minimal conductivity value does not have a universal character and corresponds to the impurity resonance energy rather than to the Dirac point position in the spectrum. The substantial asymmetry of the resulting dependence of the conductivity on the gate voltage magnitude is attributed as well to this same shift of the conductivity minimum to the resonance state energy.

PACS numbers: 71.23.-k, 71.55.-i, 81.05.Uw

## I. INTRODUCTION

Graphene, a thermodynamically stable graphite monolayer, which has been mechanically exfoliated for the first time only a few years ago,<sup>1-3</sup> is gaining considerable scientific attention. This new material looks promising enough for a number of important practical applications, some of which have been long hoped for. While experimenters are targeted at engineering graphene based devices in the not so distant future, graphene attracts theoreticians as the first existing in the free state physical system, which can be named two-dimensional (2D) without any reservations. Undoubtedly, so far unique electronic properties of graphene were the most challenging issue. These properties directly arise from the honeycomb lattice with its two-atomic structure, inherent in a single atomic layer of graphite. The lattice structure leads to the Dirac dispersion of charge carriers, which makes up the core of studies devoted to the graphene.

Transport properties of this material are, sure enough, paramount for graphene-based electronics. In real crystals, transport properties essentially depend on non-ideality of the system and on interaction of carriers with other excitations. Below we are going to focus on imperfections of graphene, and, in particular, on point defects in it. This allows to rise a question on the spectrum of delocalized carriers, on its dependence on the amount of defects, and, eventually, on such a remarkable quantity as the minimal value of the conductivity.

At the outset, two main properties of the conductivity in graphene had drawn a considerable attention. The first one was the fact that the conductivity of graphene devices never dropped below a certain value. Thus, the problem of “minimum conductivity” were coined, and the minimal value itself seemed not to vary between different experimental samples. For that reason, the origin of the universal behavior of the minimal conductivity value has been extensively searched for. The second property was the linear dependence of conductivity on the gate voltage. However, the minimum conductivity has been found soon to be strongly sample dependent,<sup>4</sup> and the effect of minimum conductivity has been attributed to graphene’s imperfections. Likewise, impurities has been credited for the linear dependence of the conductivity on the gate voltage. In this connection, a qualitative difference between charged impurities and point defects has been established.<sup>5</sup> While charged impurities are able to yield the required linear dependence, point defects were accused on producing the sub-linear conductivity, and, consequently, ruled out as the generator of the conductivity

behavior. The concept of charged impurities as a main source of the scattering mechanism in graphene has been thoroughly developed,<sup>6–8</sup> and convincingly compared to the experimental data on graphene with deposited potassium atoms on its surface.<sup>9,10</sup> At the same time, just the constant contribution to conductivity were ascribed to point defects.

Even though the concept of charged impurities looks sounding, experiments on graphene in ethanol environment seriously question the dominant role of the Coulomb scatterers.<sup>11</sup> In addition, the conductivity asymmetry evident in measurements of graphene with deposited potassium atoms has not received the proper explanation yet.<sup>9,10</sup> Moreover, the marked asymmetry of conductivity dependence on the gate voltage in graphene doped by transition metals manifests the response that is different from the one, which is expected from the charged impurity centers.<sup>12</sup> The clearly sub–linear character of conductivity curves corresponding to graphene samples heavily doped by transition metals or lightly doped by the potassium atoms only strengthen the overall impression that we are dealing with the interplay of different types of disorder, and that each one of them should receive a comprehensive treatment in effort of grasping the properties of conductivity in graphene.

Below we are returning to the common in semiconductor physics model of a binary alloy intending to examine what features of graphene’s conductivity it is capable to reproduce. Such short–range impurities violate the electron–hole symmetry of the system and are naturally allowing for the conductivity asymmetry. In contrast to former studies, we are going to show that the effective conductivity minimum corresponds not to the Dirac point of the spectrum, but to the energy of a single impurity resonance, where the impurity scattering is the strongest.

## II. MODEL DISORDERED SYSTEM

The model of massless Dirac fermions seems to be routinely employed in theoretical studies devoted to electron subsystem related physical phenomena in graphene. Despite the well–known fact that the linear dispersion domain spans, in a strict sense, only over a tiny portion of the whole spectrum, which is smaller than one tenth of the total bandwidth, this simplistic model is capable in capturing the essential physics of charge carriers in graphene. The practical sufficiency of the model comes out from the actual Fermi level position in this material. It is known that in real experimental situations the Fermi level in graphene is

located, nearly unavoidably, in a close vicinity of the Dirac point in the electron spectrum, where it can be described by the linear dispersion with a good accuracy, and the most intriguing events are unfolding inside the narrow spectral region. Since only one of the two Dirac cones of the electron spectrum in graphene is usually retained within the model of massless and spinless fermions, the resulting Hamiltonian reads,

$$\mathbf{H}_0 = \sum_{\mathbf{k}} [f(\mathbf{k})c_1^\dagger(\mathbf{k})c_2(\mathbf{k}) + f^*(\mathbf{k})c_2^\dagger(\mathbf{k})c_1(\mathbf{k})], \quad (1)$$

$$c_\alpha(\mathbf{k}) = \frac{1}{\sqrt{N}} \sum_{\mathbf{n}} e^{i\mathbf{k}\mathbf{n}} c_{\mathbf{n}\alpha}, \quad f(\mathbf{k}) = v_F(k_x + ik_y), \quad (2)$$

where  $\mathbf{n}$  runs over lattice cells,  $\alpha = 1, 2$  enumerates two sublattices of the honeycomb atomic arrangement,  $c_{\mathbf{n}\alpha}^\dagger$  and  $c_{\mathbf{n}\alpha}$  are the electron creation and annihilation operators at the respective lattice sites,  $v_F$  is the Fermi velocity,

$$v_F = \frac{\sqrt{3}at}{2}, \quad (3)$$

$a$  is the lattice constant, and  $t \approx 2.7\text{eV}$  is the magnitude of the hopping parameter for nearest neighbors in the tight-binding approximation for graphene.<sup>13</sup> Obviously, the Hamiltonian (1) provides for the linear dispersion relation,

$$E(\mathbf{k}) = \pm v_F k. \quad (4)$$

Substitutional impurities are supposed to be distributed evenly and in uncorrelated manner on lattice sites. Presence of an impurity at a given lattice site is assumed to be manifested only through a change in the respective on-site potential of the tight-binding Hamiltonian. This type of impurity perturbation fully corresponds to the conventional model of a binary alloy with a diagonal disorder, which had been extensively used in physics of real crystals, and sometimes is referred to as the Lifshitz model for historical reasons. The corresponding electron Hamiltonian for a disordered graphene has the form,

$$\mathbf{H} = \mathbf{H}_0 + \mathbf{H}_{imp}, \quad \mathbf{H}_{imp} = V_L \sum_{\mathbf{n}, \alpha} \eta_{\mathbf{n}\alpha} c_{\mathbf{n}\alpha}^\dagger c_{\mathbf{n}\alpha}, \quad (5)$$

where  $V_L$  is the deviation of the potential at the impurity site, and variable  $\eta_{\mathbf{n}\alpha}$  is unity with the probability  $c$  or zero with the probability  $(1 - c)$ , which specifies  $c$  as the impurity concentration. At this stage, it is possible to recall that actually there are two Dirac cones in real graphene. It will be seen below that for the chosen type of the impurity perturbation two

Dirac cones are acting absolutely independently from each other. This permits to improve the model a little bit by including into consideration both Dirac cones when calculating the host Green's function,

$$\mathbf{g}(E) = (E - \mathbf{H}_0)^{-1}, \quad (6)$$

which diagonal element in the site representation will be required for the subsequent analytical treatment of the impurity problem in graphene. The straightforward expression for this diagonal element reads:

$$g_{n\alpha n\alpha}(E) \equiv g_0(E) = \frac{1}{S_{BZ}} \int \frac{E}{E^2 - \tilde{E}^2(\mathbf{k})} d\mathbf{k}, \quad (7)$$

where the integration is carried over the whole Brillouin zone that has the area

$$S_{BZ} = \frac{8\pi^2}{\sqrt{3}a^2}, \quad (8)$$

and  $\tilde{E}(\mathbf{k})$  is the exact dispersion relation corresponding to the accurate  $\tilde{f}(\mathbf{k})$  instead of the approximate  $f(\mathbf{k})$  from (2) in the host Hamiltonian (1). In order to simplify the expression, as it was pointed out above, the exact dispersion relation  $\tilde{E}(\mathbf{k})$  can be replaced by two identical Dirac cones with the linear dispersion  $E(\mathbf{k})$  for the energies laying in a close vicinity of  $E = 0$ . Then, the integration in Eq. (7) over the wave vector can be performed relative to the each cone vertex,

$$g_0(E) \approx \frac{2}{S_{BZ}} \int \frac{E}{E^2 - E^2(\mathbf{k})} d\mathbf{k}, \quad (9)$$

where the factor 2 reflects the presence of two Dirac cones in the spectrum. However, the integration can not be done over the entire Brillouin zone due to the mutual overlap between cones after an approximation of this kind. The corresponding cutoff magnitude of the wave vector is determined by the sum rule,

$$\frac{4\pi}{S_{BZ}} \int_0^{k_{max}} dk = 1, \quad (10)$$

which yields

$$k_{max} = \frac{2\sqrt{\pi}}{\sqrt{\sqrt{3}a}}. \quad (11)$$

Finally, the diagonal element of the host Green's function can be obtained exactly in this approximation,

$$\begin{aligned} g_0(E) \approx \frac{4\pi}{S_{BZ}} \int_0^{k_{max}} \frac{E}{E^2 - (v_F k)^2} k dk &= \int_0^1 \frac{E}{E^2 - \sqrt{3}\pi t^2 z} dz = \\ &= \frac{\epsilon}{W} \left[ \ln \left( \frac{\epsilon^2}{1 - \epsilon^2} \right) - i\pi \operatorname{sgn} \epsilon \right], \quad E < W, \end{aligned} \quad (12)$$

where

$$W = \sqrt{\pi\sqrt{3}t}, \quad (13)$$

is the bandwidth parameter. From here and on we are choosing it as the energy unit. For the sake of clarity, we will use the dimensionless designations:

$$\epsilon = \frac{E}{W}, \quad v = \frac{V_L}{W}, \quad (14)$$

for the energy and the impurity potential correspondingly. Since the adopted approximation is valid only for energies that are small compared to the bandwidth, the proper expression for the dimensionless diagonal element of the Green's function can be easily written as:

$$g_0(\epsilon) \approx 2\epsilon \ln |\epsilon| - i\pi |\epsilon|, \quad |\epsilon| \ll 1. \quad (15)$$

### III. RENORMALIZED ENERGY PHASE AND CONDUCTIVITY

The Green's function of a disordered system,

$$\mathbf{G} = (\epsilon - \mathbf{H})^{-1}, \quad (16)$$

after averaging over different impurity distributions,  $\mathbf{G} = \langle \mathbf{G} \rangle$ , regains the translational invariance and can be expressed by means of the Dyson equation,

$$\mathbf{G} = \mathbf{g} + \mathbf{g} \Sigma \mathbf{G}, \quad (17)$$

where  $\Sigma$  is the self-energy. When amount of introduced impurities is moderate, it is possible to implement the modified propagator method.<sup>14</sup> Within this approach, the self-energy is site diagonal and identical on both sublattices,

$$\Sigma \approx \Sigma(\epsilon) \mathbf{I}, \quad \Sigma(\epsilon) = \frac{cv}{1 - vg_0[\epsilon - \Sigma(\epsilon)]}, \quad (18)$$

where  $\mathbf{I}$  is the identity matrix. At a small impurity concentration,  $c \ll 1$ , multiple occupancy corrections are not significant. Thus, the method of modified propagator yields results that are practically indistinguishable from the ones produced by the conventional coherent potential approximation. Inclusion of only single-site scattering in this approximation and the site diagonal character of the impurity perturbation accounts for the possibility to consider, as was noted above, two actual Dirac cones in the dispersion relation independently.

In order to make the self-consistency condition (18) more tractable, a regular substitution can be made,

$$\epsilon - \Sigma(\epsilon) = \varkappa \exp(i\varphi), \quad \varkappa > 0, \quad 0 < \varphi < \pi, \quad (19)$$

which singles out the phase of the renormalized energy  $\epsilon - \Sigma(\epsilon)$ . This phase diminishes from  $\pi/2$  to zero inside the conduction band and rise from  $\pi/2$  to  $\pi$  within the valence band when moving away from the Dirac point position. With the help of the obtained above expression (15) for the diagonal element of the Green's function and the substitution (19), the imaginary part of Eq. (18) can be reduced as follows,

$$\begin{aligned} cv^2 [2 \ln \varkappa + (2\varphi - \pi) \cot \varphi] + [1 - v\varkappa(2 \ln \varkappa \cos \varphi - (2\varphi - \pi) \sin \varphi)]^2 + \\ + [v\varkappa(2 \ln \varkappa \sin \varphi + (2\varphi - \pi) \cos \varphi)]^2 = 0. \end{aligned} \quad (20)$$

Provided that the impurity perturbation strength  $v$  and the impurity concentration  $c$  are fixed, this equation establishes a correspondence between the renormalized energy modulus  $\varkappa$  and its phase  $\varphi$ . For those  $\varkappa$  that are exceeding a certain threshold magnitude, which is, indeed, determined by the impurity concentration and the perturbation strength, this equation always has two different solutions with respect to the phase  $\varphi$ . One of them ( $\varphi < \pi/2$ ) belongs to the conduction band, while the other ( $\varphi > \pi/2$ ) lies within the valence band. The literal carrier energy that corresponds to a given renormalized energy is determined by the real part of Eq. (18),

$$\begin{aligned} \epsilon = \varkappa \cos \varphi + \\ + \frac{cv [1 - v\varkappa(2 \ln \varkappa \cos \varphi - (2\varphi - \pi) \sin \varphi)]}{[1 - v\varkappa(2 \ln \varkappa \cos \varphi - (2\varphi - \pi) \sin \varphi)]^2 + [v\varkappa(2 \ln \varkappa \sin \varphi + (2\varphi - \pi) \cos \varphi)]^2}. \end{aligned} \quad (21)$$

Taken together, the last two equations, (20) and (21), are making up a set, which implicitly specifies the dependence of the renormalized energy phase  $\varphi$  on the carrier energy  $\epsilon$ .

Since the procedure required to calculate the self-energy is already outlined, it is possible to employ the Kubo expression for the conductivity of a disordered graphene at the zero temperature,<sup>15</sup>

$$\tilde{\sigma}_{cond} = \frac{4e^2}{\pi h} \left\{ 1 + \left[ \frac{\epsilon_F - \text{Re } \Sigma(\epsilon_F)}{-\text{Im } \Sigma(\epsilon_F)} + \frac{-\text{Im } \Sigma(\epsilon_F)}{\epsilon_F - \text{Re } \Sigma(\epsilon_F)} \right] \arctan \left[ \frac{\epsilon_F - \text{Re } \Sigma(\epsilon_F)}{-\text{Im } \Sigma(\epsilon_F)} \right] \right\}, \quad (22)$$

where  $\epsilon_F$  is the Fermi energy. By means of the substitution (19), which was used above to simplify the self-consistency condition for the self-energy (18), the above expression can be

significantly reduced,

$$\tilde{\sigma}_{cond} = \left( \frac{e^2}{h} \right) \sigma_{cond}, \quad \sigma_{cond} = \frac{2}{\pi} \left[ 1 + (\cot \varphi_F + \tan \varphi_F) \left( \frac{\pi}{2} - \varphi_F \right) \right], \quad (23)$$

where  $\varphi_F$  is the renormalized energy phase at the Fermi level, and the dimensionless conductivity  $\sigma_{cond}$ , which will be used onwards, is singled out. It should be emphasized that the dimensionless conductivity  $\sigma_{cond}$  depends on the renormalized energy phase  $\varphi$  alone. In the same way, the well-known Ioffe–Regel criterion,<sup>16</sup> which is commonly used to separate extended states in a disordered system, and the applicability criterion of the modified propagator method can both be expressed through the same renormalized energy phase.<sup>17</sup> It has been shown that with varying the renormalized energy phase the modified propagator approximation validity violation and the indication of the state localization by the Ioffe–Regel criterion are occurring simultaneously for those states, which energies fall inside the host band of a disordered system.<sup>17,18</sup> Certainly, it is not conceptually correct to expect that the Ioffe–Regel criterion can be used to pinpoint precisely the mobility edge position in a disordered system. Similarly, there should be no sharp boundaries between those spectral regions, in which the modified propagator method is applicable, and those ones, in which it is not. Nevertheless, there are strong arguments supporting the estimation that the mobility edge in a disordered system should be located at those energy, at which the renormalized energy phase is close to  $\pi/6$  for the conduction band, and, respectively, to  $5\pi/6$  for the valence band. Thus, in those spectral intervals, inside which states are anticipated to be localized according to the Ioffe–Regel criterion, neither the Kubo formula (23) has any relevance, nor the modified propagator method is reliable. On the contrary, the approach outlined above is consistent in the spectral domains occupied with extended states, where the renormalized energy phase  $\varphi$  is either small (for the conduction band) or close to  $\pi$  (for the valence one).

## IV. CONDUCTIVITY IN DIFFERENT SCATTERING REGIMES

### A. Weak scatterers

When the impurity perturbation strength is moderate ( $|v| < 1$ ), it is possible to take an advantage of the renormalized energy phase smallness (or its closeness to  $\pi$ ) and construct

a correspondent approximate solution of Eq. (20),

$$\theta \approx \frac{\pi cv^2}{(1 \mp 2v\kappa \ln \kappa)^2 + (\pi v\kappa)^2 + 2cv^2(1 + \ln \kappa)}, \quad \theta \ll 1, \quad (24)$$

where  $\theta$  stands for  $\varphi$  inside the conduction band, and for  $\pi - \varphi$  inside the valence band. The sign in the denominator also switches from a minus to a plus when moving from the conduction band to the valence band. Obviously, the renormalized energy phase is close to  $\pi/2$  in a narrow interval of energies around the shifted Dirac point, and thus the above approximation is not valid inside this region. However, the transition of the renormalized energy phase from small values to values that are close to  $\pi$  is very fast. This transitional region is, in fact, exponentially narrow and, for certain reasons, should be treated separately, as it will be explained in detail below.

It is not difficult to check that in this scattering regime ( $|v| < 1$ ) the effective shift of states along the energy axis, which is given by the real part of the self-energy  $\text{Re } \Sigma(\epsilon)$ , is nearly constant in the whole domain under consideration ( $|\epsilon| \ll 1$ ). Therefore, as a first approximation, one can take

$$\pm \kappa \approx \epsilon - cv, \quad (25)$$

where the sign is varying according to the current band as above, so that  $\kappa$  always remains positive, as it should do. The expression for the conductivity, Eq. (23), can be also simplified utilizing the smallness (or closeness to  $\pi$ ) of the renormalized energy phase,

$$\sigma_{\text{cond}} \approx \frac{1}{\theta}, \quad \theta \ll 1, \quad (26)$$

where linear terms and terms of the higher order in  $\theta$  are omitted. All these approximations, Eqs. (24)–(26), can be combined into the final expression for the dimensionless conductivity,

$$\sigma_{\text{cond}} \approx \frac{[1 - 2v(\epsilon_F - cv) \ln |\epsilon_F - cv|]^2 + [\pi v(\epsilon_F - cv)]^2}{\pi cv^2} + \frac{2}{\pi} [1 + \ln |\epsilon_F - cv|], \quad (27)$$

which fits the conductivity, calculated numerically by Eqs. (20), (21), and (23), surprisingly well throughout the whole considered interval of energies ( $|\epsilon| \ll 1$ ).

As follows from (27), the conductivity is gradually diminishing with increasing the Fermi energy  $\epsilon_F$  from the valence band to the conduction band for a negative impurity perturbation ( $v < 0$ ) and vice versa. The conductivity of graphene calculated by Eqs. (20), (21), and (23) without any additional approximations at different concentrations of point defects is plotted against the Fermi energy in Fig. 1 for the case of moderate impurity perturbation ( $|v| < 1$ ).

On the whole, the dependence of the conductivity on the Fermi energy is smooth and almost featureless, while being strongly asymmetric against the shifted Dirac point position. The only exception from the monotonic behavior of the conductivity can be observed in a close vicinity of the Dirac point, where the curve manifests a sharp dip, which is barely discernible in the curves corresponding to high impurity concentrations. If to trust the results yielded by the modified propagator method all the way down to the Dirac point, the conductivity at its very tip should drop to  $4/\pi$ . This directly corresponds to the notorious theoretical magnitude of the universal minimum conductivity in the inhomogeneous graphene, which has been widely debated within the so-called “missed  $\pi$ ” discourse. However, the modified propagator method is not applicable in the Dirac point neighborhood. It can be shown<sup>18,19</sup> that this approximation is not reliable in the interval

$$|\epsilon - cv| \lesssim \exp\left(-\frac{1}{4cv^2} - 1\right). \quad (28)$$

Therefore, as it was outlined in the previous section, the Kubo formula is also ineffective in this interval, and the obtained conductivity magnitude at the Dirac point has no physical meaning. Still, the width of the energy interval, in which the analytical approach fails, is exponentially small compared to the bandwidth. Since the corresponding dip on the conductivity curve is so narrow, it should be averaged out at realistic sample temperature, or by means of any other broadening mechanism.

Consequently, the presence of the sharp dip on the conductivity curve can be neglected, and, probably, should never come out in actual experiments. The asymmetry of the conductivity dependence on the Fermi energy arises from the presence of the severely smeared out impurity resonance, which enhances the impurity scattering. Indeed, the smooth character of the conductivity curve does not resemble the experimentally observed check mark shape. However, if this check mark shape is caused by another dominating type of impurities, weakly scattering point defects undoubtedly can contribute to the asymmetry of the conductivity curve.

## B. Strong scatterers

In the limit of the strong impurity scattering,  $|v| \gg 1$ , situation is completely different. When the impurity potential is large compared to the bandwidth, a well-defined resonance

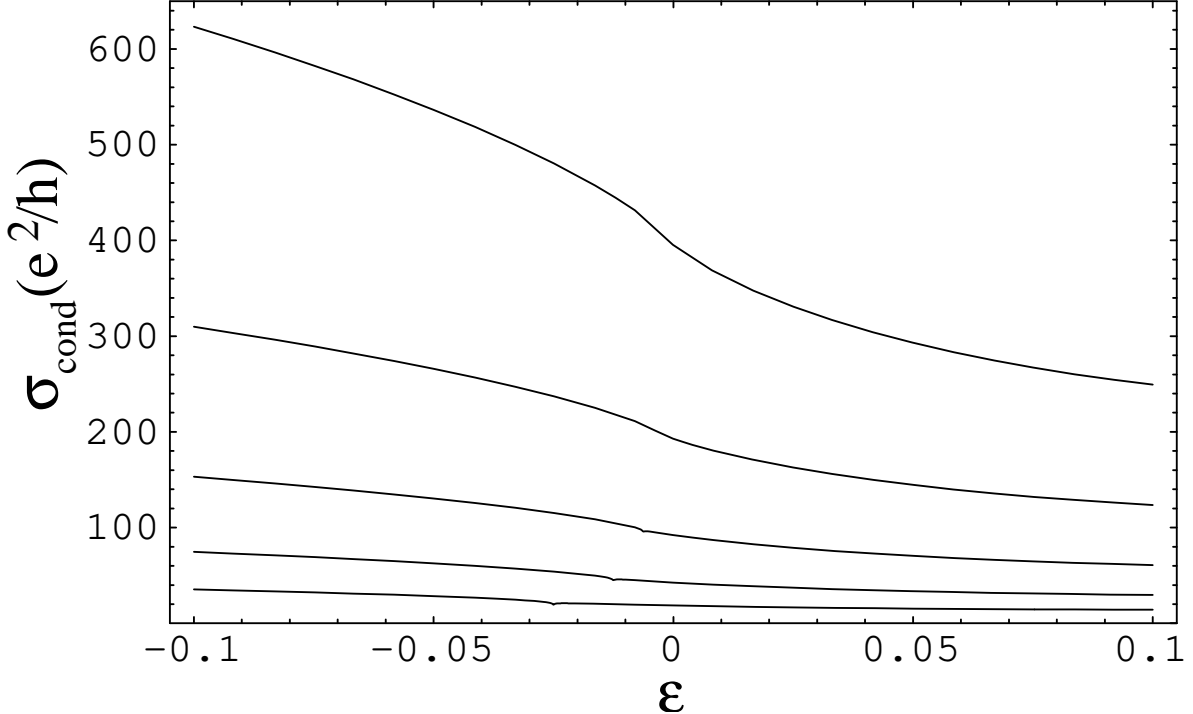


FIG. 1: Conductivity of graphene with point defects *vs* Fermi energy for  $v = -0.5$  and concentrations  $c = 0.1/2^n$ ,  $n = 1 \dots 5$ .

state is manifested in the electron spectrum.<sup>18</sup> In the limit of a strong impurity potential, the resonance state energy  $\epsilon_r$  is determined by the Lifshitz equation,

$$1 \approx v \operatorname{Re} g_0(\epsilon_r) \approx 2v\epsilon_r \ln |\epsilon_r|, \quad (29)$$

while the resonance state damping is given by

$$\Gamma_r \approx \frac{\pi |\epsilon_r|}{2|1 + \ln |\epsilon_r||}. \quad (30)$$

For the resonance state to be well-defined, the condition

$$\gamma_r \equiv \frac{\Gamma_r}{|\epsilon_r|} \approx \frac{\pi}{2|1 + \ln |\epsilon_r||} \ll 1 \quad (31)$$

must be met. Thus, one should have  $|\ln |\epsilon_r|| \gg 1$ , which corresponds to a strong impurity perturbation and a resonance energy located close to the Dirac point.

The qualitative difference of the strong impurity perturbation case resides not only on the presence of a resonance state in the spectrum, but mainly on the fact that in this case the electron spectrum undergoes a radical rearrangement. That is, with increasing impurity

concentration a quasigap filled with localized states opens up around the resonance state energy.<sup>18–20</sup> There exists a certain critical concentration of impurities,

$$c_r \sim -\frac{1}{2v^2 \ln(\zeta/|v|)}, \quad \zeta \sim 1, \quad (32)$$

which is determined by the mutual spatial overlap of individual impurity states. When impurity concentration exceeds the critical concentration  $c_r$  of the spectrum rearrangement, the width of the quasigap starts to increase rapidly with increasing impurity concentration as  $\sqrt{-2c/\ln c}$ .<sup>18–20</sup> Certainly, neither the modified propagator method nor the Kubo expression for the conductivity will work inside this quasigap. Therefore, we will consider only those impurity concentrations that are less than the critical one ( $c < c_r$ ) in the case of the strong impurity potential. Vacancies are frequently modeled by point defects with infinite impurity potentials  $v$ . Because of this, the critical concentration  $c_r$  for vacancies in graphene is zero. In other words, the spectrum rearrangement is already over for any concentration of vacancies. Therefore, vacancies are out of the scope of the present study.

The conductivity calculated directly by Eqs. (20), (21), and (23) at different concentrations of point defects is shown in Figs. 2 and 3 for a not so excessive ( $v = -2$ ) and for a reasonably strong ( $v = -8$ ) impurity potential, respectively. The Dirac point shift, which occurs along with the impurity concentration increase, is not so pronounced, because  $c_r v \sim 1/v$ . Like in the case of the weak impurity potential, there is a sharp dip in the conductivity curve located at the Dirac point. The hint of this dip can be seen in the figures at concentrations that are approaching the critical one. Nevertheless, the presence of this dip should be neglected by the same arguments as above.

What really distinguishes the strong impurity perturbation case is the presence of the clear minimum on the conductivity curve, which is located at the energy of the impurity resonance state. This is understandable, since the impurity scattering is the strongest around the resonance energy. The width of this minimum corresponds to the resonance state broadening, and, therefore, this minimum is not as sharp as the minimum at the Dirac point. Overall, the conductivity curve acquires a quasi-parabolic form, which is particularly well-pronounced at lower impurity concentrations. In addition, the conductivity curve appears more symmetric for a larger impurity potential.

With increasing the impurity concentration, the concentration broadening of the resonance state also increases. At the impurity concentrations that are close to the critical

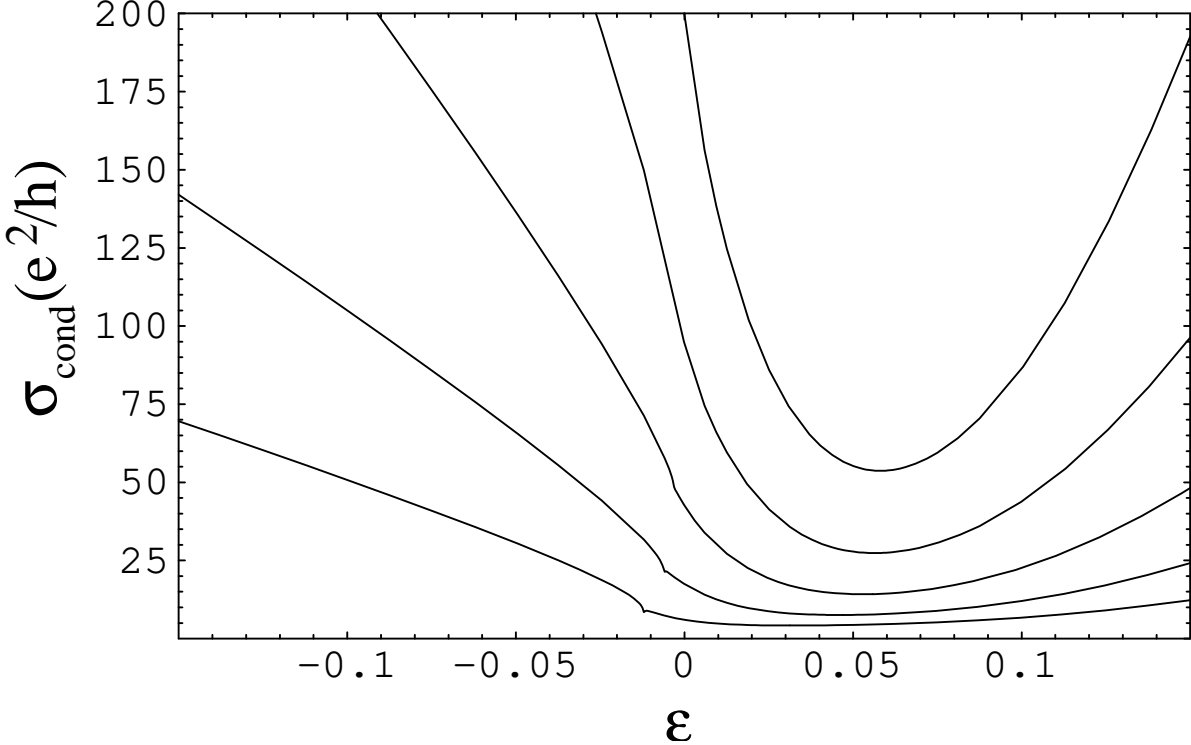


FIG. 2: Conductivity of graphene with point defects *vs* Fermi energy for  $v = -2$  and concentrations  $c = c_r/2^n$ ,  $n = 1 \dots 5$ ,  $c_r \approx 0.012$ .

one, the broadening of the resonance state is as wide as the distance from the resonance energy to the Dirac point. This widening of the resonance broadening area along with the tendency of states toward localization inside it are manifested by the apparent flattening of the conductivity curve around the resonance energy at  $c \sim c_r$ . Outside the domain of the concentration broadening, the approximate expression for the conductivity is even simpler than before,

$$\sigma_{\text{cond}} \approx \frac{[1 - 2v\epsilon_F \ln |\epsilon_F|]^2 + [\pi v \epsilon_F]^2}{\pi x v^2}. \quad (33)$$

However, this expression can not be used close to the resonance energy. In order to obtain the minimum value of the conductivity, it is required to know the magnitude of the renormalized energy phase at the resonance energy. Its concentration dependence,  $\varphi_r(c)$ , follows from the self-consistency condition (20). The second term in this equation nullifies by the very definition of the resonance energy Eq. (29). The remaining two terms constitute the relation:

$$c = -2\epsilon_r^2(c) \tan \varphi_r(c) \left[ \ln \left| \frac{\epsilon_r(c)}{\cos \varphi_r(c)} \right| \tan \varphi_r(c) + \varphi_r(c) - \frac{\pi}{2} \right]. \quad (34)$$

This expression can be significantly simplified by taking into account that introduced earlier

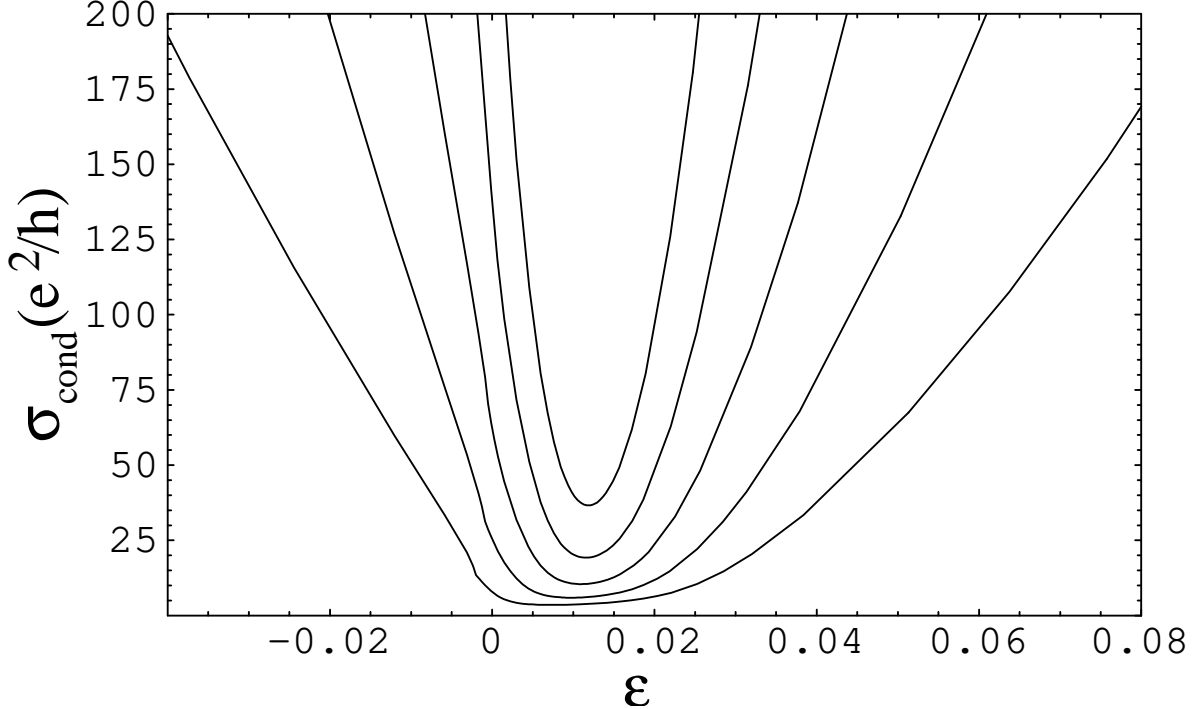


FIG. 3: Conductivity of graphene with point defects *vs* Fermi energy for  $v = -8$  and concentrations  $c = c_r/2^n$ ,  $n = 1 \dots 5$ ,  $c_r \approx 0.0005$ .

symmetric phase  $\theta$  is small at low impurity concentrations,

$$c \approx \pi \epsilon_r^2(c) \theta_r(c) \left[ 1 + \frac{\theta_r(c)}{\gamma_r} \right], \quad \theta_r(c) \ll 1. \quad (35)$$

Dependence of the resonance energy on the concentration  $\epsilon_r(c)$  is very weak for the strong impurity perturbation and can be neglected. By setting the resonance energy in Eq. (35) to its value for the isolated impurity, this equation can be solved for the renormalized energy phase at the resonance  $\theta_r$ ,

$$\theta_r(c) \approx \frac{\gamma_r}{2} \left( \sqrt{1 + 8 \frac{c}{c_r}} - 1 \right). \quad (36)$$

The minimum conductivity at the resonance energy is then given by Eq. (26). Indeed, it does not again have the universal character and varies with impurity concentration. The minimum value of conductivity calculated numerically with the help of Eqs. (20), (21) and (23) is plotted against the impurity concentration in Figs. 4 and 5 for two different values of the impurity potential. Initial fast conductivity drop with increasing the impurity concentration is followed by the considerable flattening of the curve. The manifested saturation-type behavior of the minimum conductivity concentration dynamics qualitatively corresponds to the observed data.<sup>9</sup>

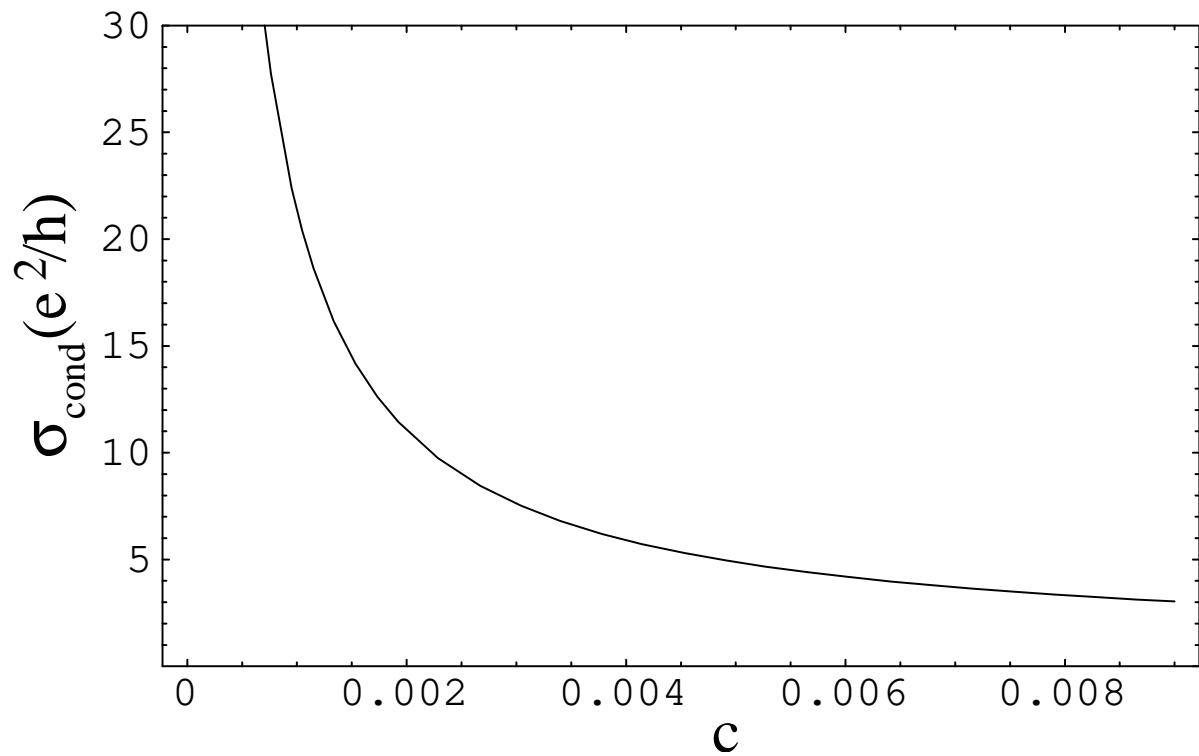


FIG. 4: The minimum conductivity *vs* impurity concentration for  $v = -2$ .

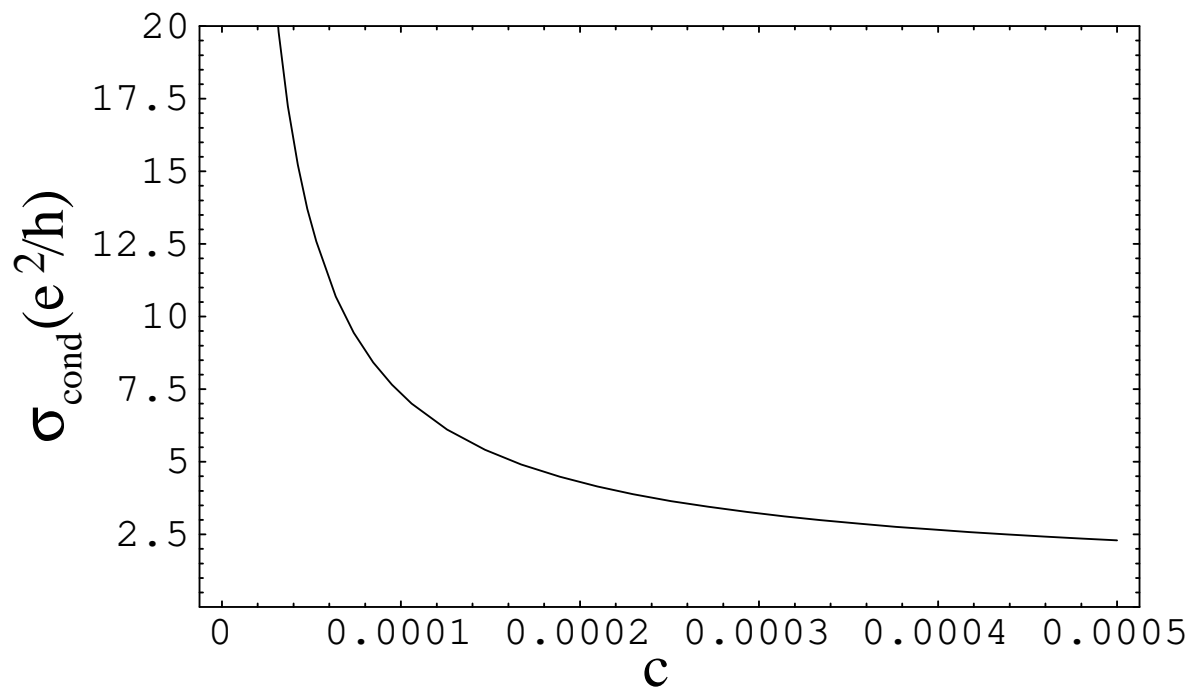


FIG. 5: The minimum conductivity *vs* impurity concentration for  $v = -8$ .

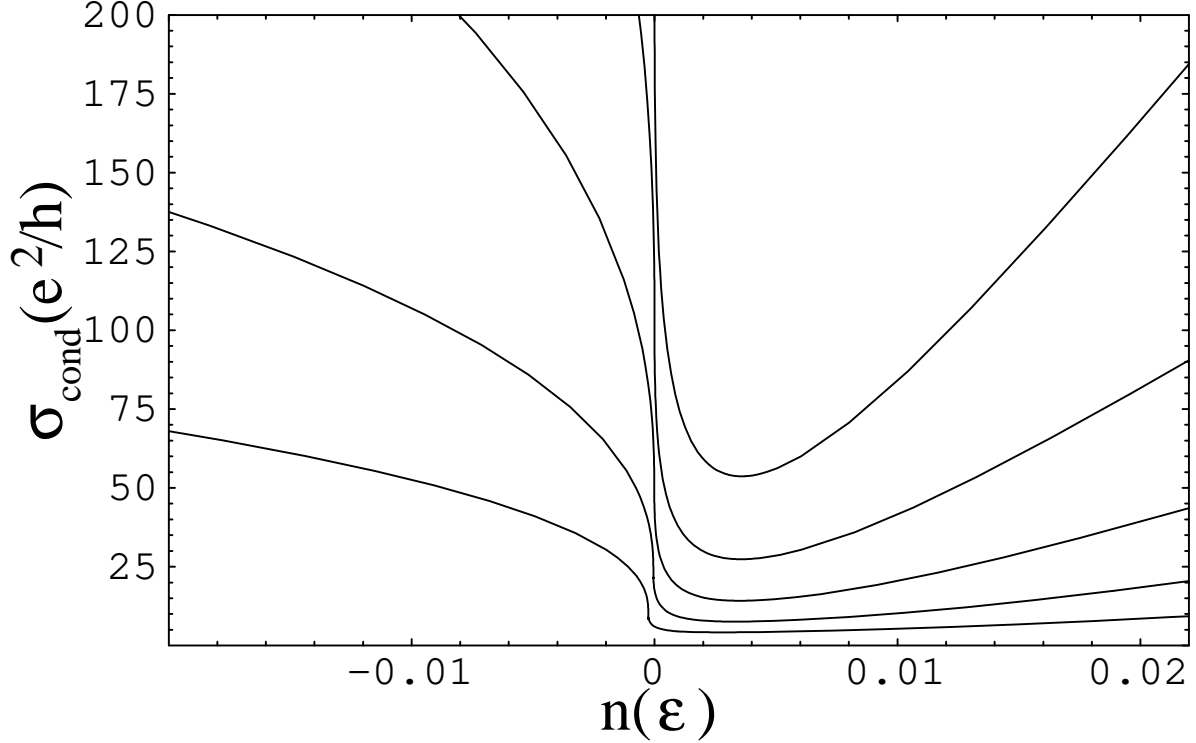


FIG. 6: Conductivity of graphene with point defects *vs* number of carriers for  $v = -2$  and concentrations  $c = c_0/2^n$ ,  $n = 1 \dots 5$ ,  $c_0 \approx 0.012$ .

## V. CONDUCTIVITY ASYMMETRY

The conductivity of graphene devices is usually measured against the applied gate voltage. Since the gate voltage controls the carrier density in the graphene sample, these experimental curves can be simulated by plotting the conductivity as a function of the number of occupied states. Leaving out the irrelevant constant, and taking into account two actual sublattices, the number of occupied states can be written as follows,

$$n(\epsilon_F) = -\frac{2}{\pi} \int_0^{\epsilon_F} \text{Im}(\{\epsilon - \Sigma(\epsilon)\} \{\ln[\epsilon - \Sigma(\epsilon)] - i\pi\}) d\epsilon. \quad (37)$$

The conductivity of impure graphene, calculated as before by Eqs. (20), (21) and (23), is plotted in Figs. 6 and 7 for both chosen strengths of impurity perturbation against the number of occupied states, which is given by Eq. (37). The number of occupied states is calculated by the numerical integration.

It immediately strikes the eyes that the simulated conductivity dependence on the gate voltage is highly asymmetric. Similar asymmetric character of the conductivity curve has

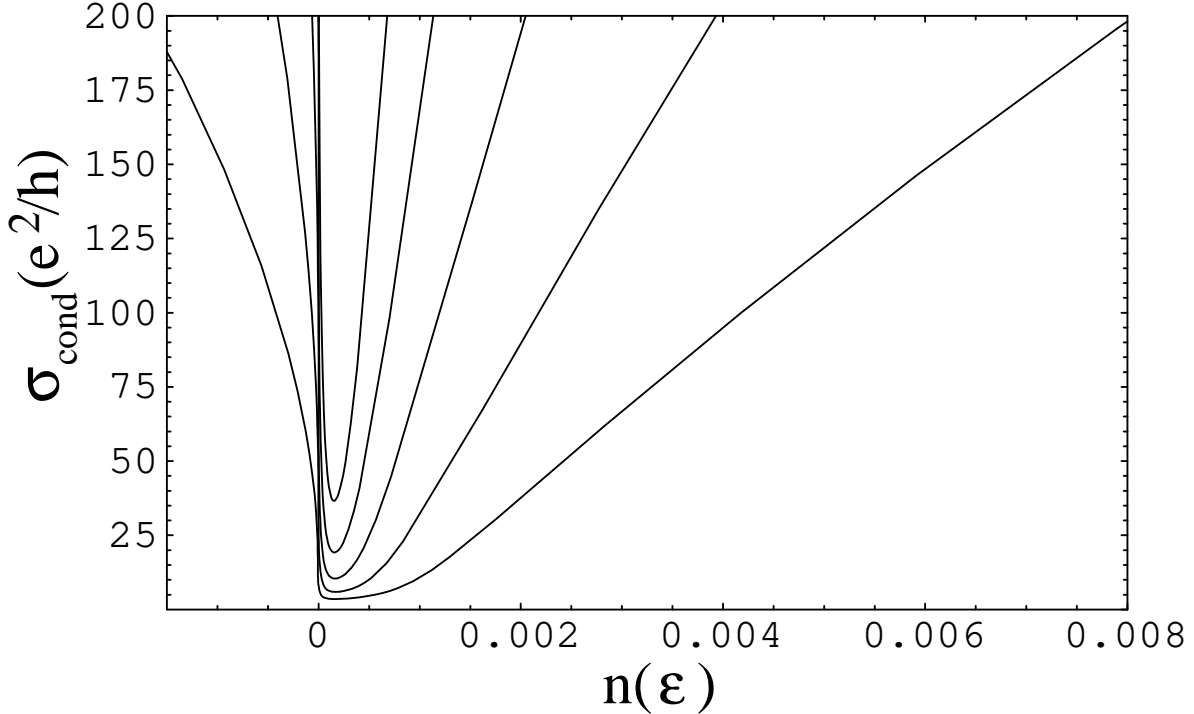


FIG. 7: Conductivity of graphene with point defects *vs* number of carriers for  $v = -8$  and concentrations  $c = c_0/2^n$ ,  $n = 1 \dots 5$ ,  $c_0 \approx 0.0005$ .

been already reported elsewhere for the graphene with point defects.<sup>21</sup> While the expected slightly sublinear behavior of the impure graphene conductivity is readily reproduced, the asymmetry of the curve appears to be bit on the extreme side. Although such a strong asymmetry is sometimes reported for a graphene with deposited adatoms,<sup>12</sup> its cause is to be understood. In order to proceed in this direction, the conductivity can be expanded into a series about its minimum. Since it has been reasoned above that the conductivity reaches its minimum value at the resonance energy  $\epsilon_r$  for the strong impurity perturbation, the expansion is straightforward,

$$\sigma_{cond} \approx \sigma_{cond}^0 + \beta(\epsilon_F - \epsilon_r)^2, \quad \beta > 0 \quad (38)$$

where  $\sigma_{cond}^0$  is the minimum value of the conductivity, and  $\beta$  is some constant.

In the current paper we restrict ourselves for the strong scattering regime to those impurity concentrations that are less than the critical concentration  $c_r$  of the spectrum rearrangement. In this case, the density of states is not considerably distorted by the presence of defects. Because of the estimative character of this arithmetic, it is quite sufficient to assume that the density of states remains completely unchanged, i.e. identical to the host

system, except of the rigid shift of both bands to a new Dirac point  $\epsilon_D$ ,

$$V^g \approx V_D^g + \gamma(\epsilon_F - \epsilon_D)^2 \operatorname{sgn}(\epsilon_F - \epsilon_D), \quad \gamma > 0, \quad (39)$$

where  $V_D^g$  is those magnitude of the gate voltage  $V^g$ , at which the Fermi level comes to the Dirac point of the spectrum, and  $\gamma$  is some constant. This equation can be easily solved for the Fermi energy,

$$\epsilon_F \approx \epsilon_D + \sqrt{\frac{|V^g - V_D^g|}{\gamma}} \operatorname{sgn}(V^g - V_D^g). \quad (40)$$

Substituting this result to the expansion (38), one can obtain:

$$\sigma_{cond} \approx \sigma_{cond}^0 + \frac{\beta}{\gamma} \left[ \sqrt{|V^g - V_D^g|} \operatorname{sgn}(V^g - V_D^g) - \sqrt{\gamma}(\epsilon_r - \epsilon_D) \right]^2. \quad (41)$$

It is not difficult to see, that the conductivity asymmetry arise from the shift expressed by the second term in the square brackets. If the conductivity reaches its minimum precisely at the Dirac point, then the conductivity dependence on the Fermi energy is linear and symmetric. However, we have demonstrated that the conductivity minimum is attained at the impurity resonance energy, which is essentially different from the Dirac point energy. Namely this difference does form the ground for the substantial conductivity asymmetry.

## VI. CONCLUSION

It is demonstrated that there are two scattering regimes, which characterize the behavior of the conductivity in graphene with point defects. In the weak scattering regime, i.e. when the impurity perturbation strength is less than the bandwidth, the dependence of the conductivity on the Fermi energy is monotonic and asymmetric, which can contribute to the observed conductivity asymmetry, when point defects does not dominate other sources of scattering. However, in the strong scattering regime, i.e. when the impurity potential exceeds the bandwidth, the conductivity caused by point defects manifests a distinctive minimum in its dependence on the Fermi energy. This minimum, in contrast to a majority of anticipations, corresponds not to the Dirac point of the spectrum, but to the impurity resonance energy. In this regime the asymmetry of the conductivity is evident. What is more, the pronounced asymmetry of the corresponding dependence of the conductivity on the gate voltage is caused by the very shift of the conductivity minimum from the Dirac point to

the impurity resonance energy. Despite the basic quality of the considered impurity model, it can capture the essential features of the impure graphene conductivity manifested in experiments. Thus, one can expect that increasing the number of parameters characterizing the point defect will permit to approach closer to the explanation of conductivity features in graphene with point defects.

### Acknowledgments

Authors are grateful to V. P. Gusynin for valuable discussions. This work was supported by the SCOPES grant  $\mathcal{N}^{\circ}$  IZ73Z0-128026 of Swiss NSF, by the SIMTECH grant  $\mathcal{N}^{\circ}$  246937 of the European FP7 program, and by the Program of Fundamental Research of the Department of Physics and Astronomy of the National Academy of Sciences of Ukraine.

---

<sup>1</sup> K. S. Novoselov, A. K. Geim, S. V. Morozov, D. Jiang, Y. Zhang, S. V. Dubonos, I. V. Grigorieva, and A. A. Firsov, *Science* **306**, 666 (2004).

<sup>2</sup> K. S. Novoselov, A. K. Geim, S. V. Morozov, D. Jiang, M. I. Katsnelson, I. V. Grigorieva, S. V. Dubonos, and A. A. Firsov, *Nature* **438**, 197 (2005).

<sup>3</sup> Y. Zhang, Y.-W. Tan, H. L. Stormer, and P. Kim, *Nature* **438**, 201 (2005).

<sup>4</sup> Y.-W. Tan, Y. Zhang, K. Bolotin, Y. Zhao, S. Adam, E. H. Hwang, S. Das Sarma, H. L. Stormer, P. Kim, *Phys. Rev. Lett.* **99**, 246803 (2007).

<sup>5</sup> K. Nomura, A. H. MacDonald, *Phys. Rev. Lett.* **98**, 076602 (2007).

<sup>6</sup> E. H. Hwang, S. Adam, S. D. Sarma, *Phys. Rev. Lett.* **98**, 186806 (2007).

<sup>7</sup> V. Galitski, S. Adam, S. Das Sarma, *Phys. Rev. B* **76**, 245405 (2007).

<sup>8</sup> S. Adam, E. H. Hwang, E. Rossi, S. Das Sarma, *Solid State Commun.* **149**, 1072 (2009).

<sup>9</sup> J.-H. Chen, C. Jang, S. Adam, M. S. Fuhrer, E. D. Williams, M. Ishigami, *Nature Phys.* **4**, 377 (2008a).

<sup>10</sup> J.-H. Chen, C. Jang, M. Ishigami, S. Xiao, W. G. Cullen, E. D. Williams, M. S. Fuhrer, *Solid State Commun.* **149**, 1080 (2009).

<sup>11</sup> L. A. Ponomarenko, R. Yang, T. M. Mohiuddin, M. I. Katsnelson, K. S. Novoselov, S. V. Morozov, A. A. Zhukov, F. Schedin, E. W. Hill, and A. K. Geim, *Phys. Rev. Lett.* **102**, 206603

(2009).

- <sup>12</sup> K. Pi, K. M. McCreary, W. Bao, Wei Han, Y. F. Chiang, Yan Li, S.-W. Tsai, C. N. Lau, and R. K. Kawakami, Phys. Rev. B **80**, 075406 (2009).
- <sup>13</sup> S. Reich, J. Maultzsch, C. Thomsen, and P. Ordejón, Phys. Rev. B **66**, 035412 (2002).
- <sup>14</sup> R. W. Davies, J. S. Langer, Phys. Rev. **131**, 163 (1963).
- <sup>15</sup> Hideki Kumazaki and Dai S. Hirashima, J. Phys. Soc. Jpn. **75**, 053707 (2006).
- <sup>16</sup> A. F. Ioffe and A. R. Regel, Prog. Semicond. **4**, 237 (1960).
- <sup>17</sup> Yuriy Skrypnyk, Phys. Rev. B **70**, 212201 (2004).
- <sup>18</sup> Yu. V. Skrypnyk and V. M. Loktev, Phys. Rev. B **73**, 241402(R) (2006).
- <sup>19</sup> Yu. V. Skrypnyk and V. M. Loktev, Low Temp. Phys. **33**, 762 (2007).
- <sup>20</sup> S. S. Pershoguba, Yu. V. Skrypnyk, and V. M. Loktev, Phys. Rev. B **80**, 214201 (2009).
- <sup>21</sup> T. Stauber, N. M. R. Peres, and A. H. Castro Neto, Phys. Rev. B **78**, 085418 (2008).